

EXPERIMENTAL AND NUMERICAL ANALYSIS OF THERMO-CHEMICAL EROSION IN GUN STEEL

by

**Narimane REZGUI^{a*}, Dejan M. MICKOVIĆ^b, Saša Ž. ŽIVKOVIĆ^c,
and Ivana B. IVANOVIĆ^d**

^aMilitary Academy, Belgrade, Serbia

^bFaculty of Mechanical Engineering, University of Belgrade, Belgrade, Serbia

^cMilitary Technical Institute, University of Belgrade, Belgrade, Serbia

^dInnovation Center of the Faculty of Mechanical Engineering,
University of Belgrade, Belgrade, Serbia

Original scientific paper

<https://doi.org/10.2298/TSCI180608194R>

Various factors of thermo-chemical erosion process in gun steel were analysed. The factors are mainly related to the thermal load of gun barrel inside surface, characteristics of barrel surface and chemical interactions between propellant combustion products and barrel surface. The experimental simulation of conditions in gun barrel was carried out by vented vessel firings in the device based on modification of 37 mm M39 gun. The nozzle mass loss during firing was the measure of gun steel erosion. The main thermal factor of erosion is maximum nozzle inner surface temperature. This temperature was determined experimentally by micro thermocouples measurements at specified distance away from the inner surface and by numerical analysis of the inverse heat conduction problem. Modelling of two-phase flow of propellant combustion products and unburned propellant grains in the vented vessel and heat transfer to the nozzle were conducted using developed 1-D interior ballistic code and CFD simulation in FLUENT. Influence of different propellants, TiO₂/wax wear reducing liner and tungsten-disulfide nanoparticles layer on nozzle erosion was analysed. Good agreement between experimental and computational results was achieved.

Key words: thermocouples, heat transfer, gun steel, interiorballistics, CFD, nanoparticles

Introduction

Thermo-chemical erosion in gun steel is defined as the progressive damage of the bore surface and enlargement of the bore of a gun barrel by firing, ultimately resulting in loss in the muzzle velocity, range, and accuracy and therefore the effectiveness of the weapon. Although much progress has been made towards understanding the causes of wear in gun barrels, it is still a significant problem for most types of gun. An excellent introduction to wear and erosion in gun barrels was given in [1-3]. More recent achievements were summarized in [4, 5].

The barrel erosion is the complex physical process that depends on many factors. The major contributors to wear and erosion of gun barrels are usually divided in three general groups: thermal factors, chemical factors, and mechanical factors. These factors are mainly related to thermal load of barrel interior surface, mechanical characteristics of barrel surface

* Corresponding author, e-mail: rezguinarimane@gmail.com

and chemical interaction between propellant combustion products. The relative contributions of these factors vary from system to system. However, thermal and chemical effects are generally considered to be the dominant factors.

Various laboratory devices were developed for investigations of influence factors on gun barrel erosion. One such device based on modification of 37 mm M39 gun was developed in the Military Technical Institute, Belgrade [6] and modified later to enable temperature measurements [7]. The schematic drawing and photograph of this device are presented in fig. 1.

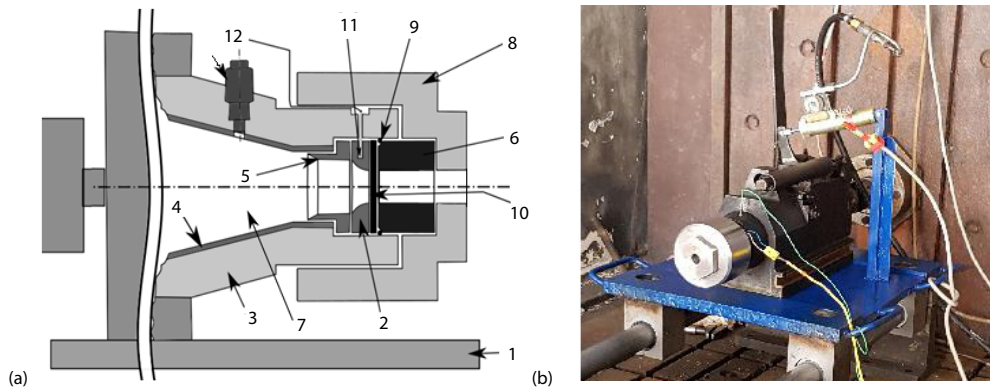


Figure 1. (a) Scheme of erosion device: 1 – base plate, 2 – nozzle, 3 – barrel, 4 – cartridge, 5 – retaining, 6 – distancer, 7 – propellant charge, 8 – disc tightener, 9 – O-ring, 10 – bursting disc, 11 – thermocouple, 12 – piezo-transducer; (b) photograph of erosion device

The main device element is the nozzle made of gun steel. Weighing the nozzle before and after firings enables the eroded mass loss to be calculated. The mean nozzle mass loss for the group of firings represents the erosivity of examined propellant charge/nozzle system. Experimental results obtained in the device can be used for estimation of gun tube erosion, because conditions in the device (determined by the mass of propellant and thickness of bursting disc) are similar to the conditions during interior ballistic cycle in the gun.

In this paper, the influence of propellant type, tungsten-disulfide nanoparticles layer on the nozzle surface and presence of TiO_2 /wax wear reducing liner in the propellant charge on nozzle erosion was analysed.

Experimental investigations

Specially profiled nozzles made of 25CrMo4 (Č 4730) gun steel with surface hardness of 25 HRC were used in experiments. The profile was defined to obtain the streamline nozzle contour.

Two types of propellants: single base propellant (NC) and single base propellant with 9.75% of dinitrotoluene (NCD) were analysed. Both propellants are in the form of 7-perforated cylindrical grains with main characteristics given in tab. 1.

Table 1. Main characteristics of propellants

| Propellant | Diameter [mm] | Perforation [mm] | Length [mm] | $(T_f)_{pr}$ [K] | f_{pr} [Jkg^{-1}] |
|------------|---------------|------------------|-------------|------------------|--------------------------------|
| NC | 6.6 | 0.65 | 14.6 | 3061 | 1032000 |
| NCD | 7.0 | 0.60 | 16.6 | 2513 | 930000 |

For experimental determination of the nozzle surface temperature micro thermocouples are embedded at a distance of approximately 1 mm from the nozzle inner surface in order that the entire heating cycle is completed before the achievement of maximum temperature at this depth. In all nozzles thermocouple wells were installed to receive a thermocouple probe. Each well was bottom-drilled to a measured distance from the inside nozzle surface. The K-type thermocouples, Nickel-Chromium/Nickel-Alumel are produced by the technology developed at the Faculty of Mechanical Engineering, Belgrade [7, 8]. The time constant of the interior ballistic cycle in erosion device is of the order of 10^{-2} second. Adopting the thermocouple time constant to be for the order of magnitude smaller than the characteristic time of the phenomenon, the sensor measuring wires of 0.025 mm diameter were used. Characteristic thermocouple recordings for firings with NC and NCD propellant are presented in fig. 2.

For experimental determination of nozzle inside surface temperature inverse heat conduction method has to be applied. A non-linear unidirectional space marching inverse conduction finite-difference algorithm presented in [9, 10] was used. Starting point is the equation of heat conduction through the nozzle wall:

$$\frac{\partial T}{\partial t} = \frac{\partial}{\partial X} \left[\alpha_n(T) \frac{\partial T}{\partial X} \right] \quad 0 < x < l_{th}, \quad t > 0 \quad (1)$$

Equation (1) is a simplification of the real physical situation because the terms arising from cylindrical symmetry are neglected. The nozzle steel thermal diffusivity:

$$\alpha_n(T) = \frac{\lambda_n(T)}{\rho_n c_n(T)} \quad (2)$$

defined from thermal conductivity and specific heat dependence on temperature [11, 12]:

$$\lambda_n(T) = \begin{cases} 48.0 \exp\left(-\frac{T}{3200}\right) [\text{Wm}^{-1}\text{K}^{-1}] & T < 773 \text{ K} \\ 76.3 \exp\left(-\frac{T}{1080}\right) [\text{Wm}^{-1}\text{K}^{-1}] & 773 \text{ K} \leq T \leq 1041 \text{ K} \\ 29.1 & T > 1041 \text{ K} \end{cases} \quad (3)$$

$$C_n(T) = 350 \exp\left(\frac{T}{1120}\right) [\text{Jkg}^{-1}\text{K}^{-1}] \quad (4)$$

Equation (1) must satisfy the following initial condition:

$$T(x, 0) = T_0 \quad (5)$$

and boundary conditions:

$$T(l_{th}, t) = m(t)$$

$$T(0, t) = T_w(t) = f(t) \quad (6)$$

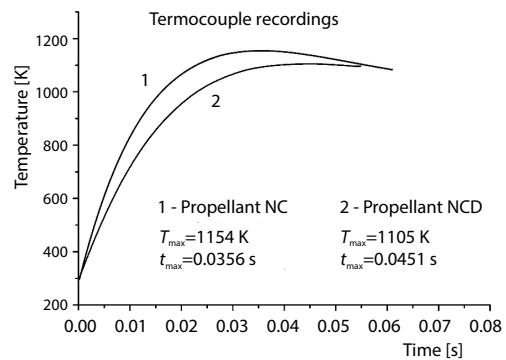


Figure 2. Thermocouple recordings for firings with NC and NCD propellant

The task of inverse method is to determine the temperature history at the inside wall, $f(t)$, starting from the temperature history at distance, l_{th} , (thermocouple location), $m(t)$. The solution procedure of the inverse problem is presented in [13]. In order to obtain stabilised inversion the choice of time step Δt [s] was made according to the following criterion for non-dimensional time step Δt^* :

$$\Delta t^* = \frac{\alpha_n(T) \Delta t}{l_{th}^2} > 0.01 \quad (7)$$

The space step Δx was chosen as to respect the *mesh Fourier number*, M_F , [14]:

$$M_F = \frac{\alpha_n(T) \Delta t}{\Delta x^2} > 1 \quad (8)$$

For stable procedure the time step $\Delta t = 0.0015$ second and space step $\Delta x = 10 \mu\text{m}$ were applied.

Four groups of five rounds were fired from the erosion device. The gas pressure in the combustion chamber was measured using a Kistler gauge. The instant of disk burst was recorded by photo-diode which records the appearance of flame at the exit of device. The propellant charge mass and bursting disk thickness were selected to obtain maximum pressure of about 320 MPa. Two 1.5 mm aluminum disks were used to provide burst pressure around 280 MPa.

Main experimental results are presented in tab. 2.

Table 2. Main experimental results in erosion device

| Group | Propellant | m_{pr} [kg] | m_{wRA} [kg] | Nozzle surface | p_{max} [MPa] | m_{ER} [mg] | $T_{w,max}$ [K] |
|-------|------------|---------------|----------------|----------------|-----------------|---------------|-----------------|
| A | NC | 0.18 | – | steel | 315.1 | 117 | 1576 |
| B | NC | 0.18 | – | WS2 layer | 300.7 | 116.5* (90) | 1569* (1440) |
| C | NCD | 0.22 | – | steel | 334.9 | 172.5 | 1524 |
| D | NCD | 0.22 | 0.0255 | steel | 334.7 | 98.0 | 1384 |

*Mean value without first round; value for first round in parentheses

Group B was fired with nozzle covered by the layer of tungsten disulfide (WS2) nanoparticles. Propellant charges in group D contained a TiO_2 /wax wear reducing additive. Experimental results given in tab. 2 will be used in this paper to analyse the influence of propellant type, tungsten-disulfide nanoparticles layer on nozzle surface and presence of TiO_2 /wax wear reducing additive in propellant charge on nozzle erosion.

Simulation of interior ballistic cycle in vented vessel

Simulation of propellant combustion products flow and heat transfer to the nozzle during interior ballistic cycle in erosion device were carried out by NERN computer code and by commercial FLUENT program [15].

Simulation of combustion products flow

The NERN code calculation

A classical interior ballistic model with heat transfer is incorporated in NERN computer code. This code represents an improvement of NERT computer code [16] reported in [13]. Main improvements are:

- Thermal characteristics of propellant gases dependent on temperature are applied.
- Radiative heat transfer to the nozzle is included.

– During combustion in closed volume the gas temperature is obtained from the mixture of igniter and main propellant combustion products.

According to the Noble-Abel equation of state the following expression applies for propellant gases during interior ballistic cycle in erosion device:

$$m_{pr}(\psi - \eta)T_g \frac{\mathfrak{R}}{M} = p \left[W_0 - \frac{m_{pr}}{\rho_{pr}}(1 - \psi - \zeta) - m_{pr}\beta(\psi - \eta) \right] \quad (9)$$

Assuming that gaseous combustion products are infinite heat source the gas temperature during combustion in closed volume (before disk burst) is:

$$T_g = \frac{m_i c_{p,i} T_{f,i} + m_{pr} \psi \bar{c}_{p,pr} T_{f,pr}}{m_i c_{p,i} + m_{pr} \psi \bar{c}_{p,pr}} \quad (10)$$

In eq. (9) $\bar{c}_{p,pr}$ is the mean specific heat of propellant between $T_{f,pr}$ and T'_g , where T'_g – the mixture temperature from the previous time step. Specific heat of igniter is supposed to be constant and equal to the flame temperature value. Black powder was used as igniter in rounds fired from erosion device ($m_i = 5$ g, $c_{p,i} = 1803$ Jkg⁻¹K⁻¹, $T_{f,i} = 1689$ K). Energy equation is:

$$\frac{f_i m_i + f_{pr} m_{pr}(\psi - \eta)}{\kappa - 1} \frac{p \left[W_0 - \frac{m_{pr}}{\rho_{pr}}(1 - \psi - \zeta) - m_{pr}\beta(\psi - \eta) \right]}{\kappa - 1} = Q_{car} + Q_{noz} \quad (11)$$

The flowing out of two-phase reactive flow through the nozzle is included in the model. Mass-flow rate of two-phase mixture through the nozzle is:

$$\dot{m}_m = \left[\kappa_m \left(\frac{2}{\kappa_m + 1} \right)^{\frac{\kappa_m + 1}{\kappa_m - 1}} \frac{1}{R_m T_g} \right] p \frac{d^2 \pi}{4} \quad (12)$$

where

$$\kappa_m = \frac{(1 - \gamma)c_p + \gamma c_{pr}}{(1 - \gamma)c_v + \gamma c_{pr}}, \quad \gamma = \frac{1 - \psi - \zeta}{1 - \eta - \zeta}, \quad R_m = \frac{\mathfrak{R}}{M}(1 - \gamma)$$

Velocity of mixture in the nozzle throat is given by expression:

$$v_m = \sqrt{(1 - \gamma) \frac{2 \kappa_m}{\kappa_m + 1} \frac{R_m T_g}{M}} \quad (13)$$

Mass fractions of propellant gases and unburned propellant grains flowing out through the nozzle are given by differential equations:

$$d\eta = \frac{(1 - \gamma)\dot{m}_m}{m_{pr}} dt \quad (14)$$

$$d\zeta = \frac{\gamma \dot{m}_m}{m_{pr}} dt \quad (15)$$

Mass fraction of burned propellant is defined by the shape and dimensions of propellant grain and by propellant burning law $r = r(p)$:

$$d\psi = \frac{S}{V_0} r(p) dt \quad (16)$$

The Runge-Kutta method for integration of differential equations was used in NERN code. The time step 10^{-5} second was used in computations. The burning surface area of 7-perforated propellant grains is calculated exactly to take slivering into account.

Specific heat at constant pressure dependence on temperature of combustion products is obtained from thermo-chemical calculations of propellant under standard conditions [17]. Composition of significant propellant combustion products calculated by thermo-chemical calculations (TCC) code is given in tab. 3.

Table 3. Composition of significant propellant combustion products calculated by TCC code

| Propellant | CO ₂ [molkg ⁻¹] | CO [molkg ⁻¹] | H ₂ O [molkg ⁻¹] | H ₂ [molkg ⁻¹] | N ₂ [molkg ⁻¹] |
|------------|--|---------------------------|---|---------------------------------------|---------------------------------------|
| NC | 4.63 | 17.13 | 9.80 | 4.35 | 4.57 |
| NCD | 2.41 | 22.42 | 6.75 | 8.43 | 4.50 |

Starting from mass fractions of gases and using specific heat dependence on temperature of individual gases the following dependence for NC and NCD propellant combustion products are obtained:

$$\text{NC propellant: } c_p(T_g) = 0.1092T_g + 1488 \text{ [Jkg}^{-1}\text{K}^{-1}\text{]}$$

$$\text{NCD propellant: } c_p(T_g) = 0.1059T_g + 1533 \text{ [Jkg}^{-1}\text{K}^{-1}\text{]} \quad (17)$$

The CFD simulation

The commercial software FLUENT was applied for simulation of a combustion products flow. The conservation equations of mass, momentum and energy were solved. The second order upwind scheme was used for discretization and the SIMPLE algorithm was employed for pressure-velocity coupling. Ballistic relations based on propellant characteristics (propellant burning rate, form function of propellant grain, real gas equation of state) are incorporated into FLUENT code as the user define function. Flow domain geometry model reproduced internal shape of the cartridge case and nozzle. Geometry model of erosion device with computational grid is given in fig. 3.

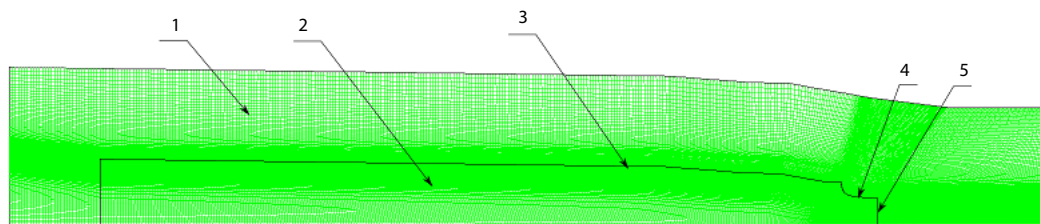


Figure 3. Geometry model of erosion device with computational grid; 1 – barrel, 2 – propellant charge, 3 – cartridge case, 4 – nozzle, 5 – Bursting disk

Structural 2-D axisymmetric mesh consisted of 135000 cells. Fine mesh was acquired in the vicinity of inner walls to ensure the correctness of the computation, fig. 4. Obtained numerical results were independent of the grid for greater number of cells.

The same thermo-chemical characteristics of combustion products as in NERN code were used. The RNG $k-\varepsilon$ turbulence model with scalable wall functions was used during both parts of calculation: combustion in constant volume, and flow through the nozzle after bursting of the disk [18].

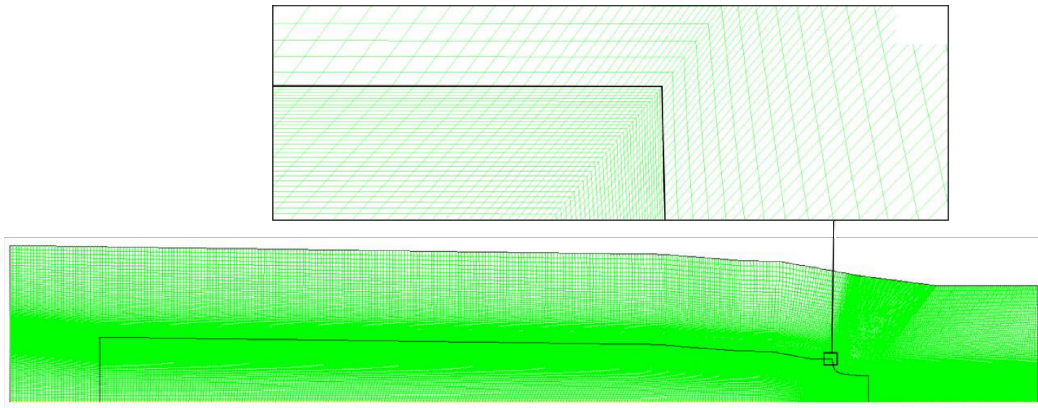


Figure 4. Boundary-layer mesh

As an example, the pressure field in the erosion device after bursting of disk (at 2.85 ms) for firing of round with NC propellant charge is given in fig. 5

Measured and calculated pressure profiles during interior ballistic cycle of rounds with NC and NCD propellant are presented in fig. 6

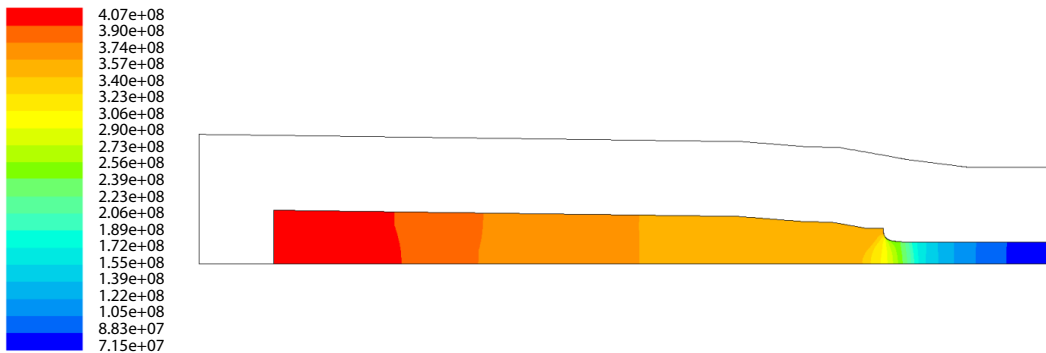


Figure 5. Pressure field calculated by FLUENT at 2.85 ms for firing of round with NC propellant charge

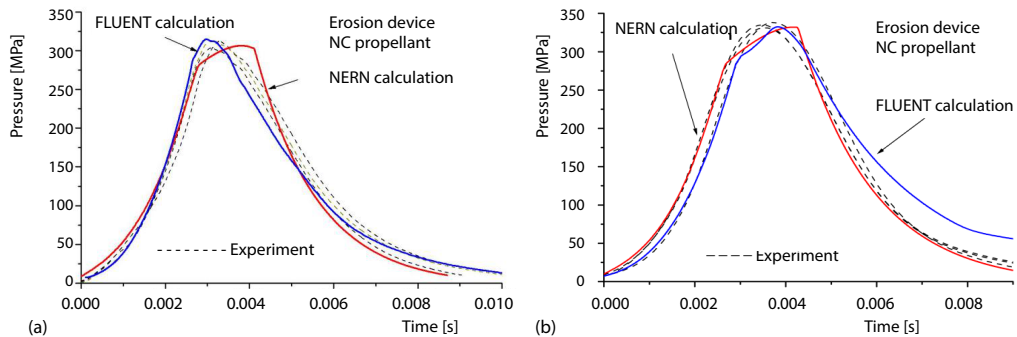


Figure 6. Experimental and calculated pressure profiles during firings of rounds; (a) with NC propellant, and (b) NCD propellant in erosion device

The NERN code results are very close to the measured pressures for NC and NCD propellant combustion in closed volume up to disk burst and for gas-flow through the nozzle (descendent part of curves). However, there is a slight difference of shape between calculated and measured pressure profiles for two-phase reactive flow through the nozzle. The two-phase mixture approach has been successfully applied in many cases for uniform distribution of very fine solid particles in the flow.

This approach is not perfectly adapted to the two-phase reactive flow in erosion device where coarse particles of burning propellant grains flow through the nozzle. This fact together with common assumptions used in classical interior ballistic models caused observed differences.

A very good agreement of FLUENT computational results with measured pressures is obtained for whole interior ballistic cycle of NC propellant charge in erosion device. However, there is a difference of shape between descendent parts of calculated and measured pressures during firings of rounds with NCD propellants. A considerably greater part of NCD propellant charge is expelled through the nozzle in the form of solid particles compared to the NC propellant charge. In FLUENT calculations only gas flow through the nozzle is considered after bursting of disk.

Simulation of heat transfer to the nozzle

The NERN code calculation

During interior ballistic cycle in erosion device the heat is transferred to the nozzle surface mainly by convection from hot propellant gases. The heat transfer by radiation is also present because of very high gas temperature.

The thermal wave depth is the approximate distance that the heat would penetrate in a given time. It is a function of the thermal diffusivity of the nozzle material [19]:

$$\delta = \sqrt{12 t \alpha_n (T)} \quad (18)$$

Duration of firing in erosion device is about 10 ms, (see figs. 6 and 7). The thermal wave depth is very small and is far from reaching the nozzle outer surface, so that the nozzle curvature and heat diffusion along the nozzle length can both be neglected. That is why the heat transfer is treated as 1-D unsteady heat conduction through the semi-infinite flat wall. In that way an analytical solution of temperature variation can be achieved with very small error [20]. Such an approach was reported in [21] for the gun barrel wall.

The heat conduction equation is:

$$\frac{\partial T(x,t)}{\partial t} = \alpha_n (T) \frac{\partial^2 T(x,t)}{\partial X^2} \quad (19)$$

with the boundary conditions:

$$-\lambda_n (T) \frac{\partial T_w(t)}{\partial t} = q_c + q_r \quad (20)$$

$$-\lambda_n (T) \left[\frac{\partial T(x,t)}{\partial t} \right]_{x \rightarrow \infty} = 0 \quad (21)$$

The convective and radiative heat fluxes are given by:

$$q_c = h [T_g - T_w(t)] \quad (22)$$

$$q_r = \varepsilon_w \sigma_{SB} [T_g^4 - T_w^4(t)] \quad (23)$$

The coefficient of convective heat transfer is estimated by the relation for turbulent pipe flow [22]:

$$h = \frac{\lambda_g(T_g)}{D_h} (3.65 + 0.0243 \text{Re}^{0.8} \text{Pr}^{0.4}) \quad (24)$$

This relation is based on a hydraulic Reynolds number to account for the presence of the solid phase:

$$\text{Re} = \frac{\rho_g v_m D_h}{\mu_g(T_g)} \quad (25)$$

The hydraulic diameter is related to the nozzle throat diameter by [23]:

$$D_h = \phi d \left(1 + \phi \frac{d}{d_{eq}} \right) \quad (26)$$

where

$$\phi = 1 - \frac{m_{pr}(1 - \psi - \zeta)}{\rho_{pr} W_0}, \quad d_{eq} = 6 \frac{V}{S}$$

Prandtl numbers is:

$$\text{Pr} = \frac{\mu_g(T_g) c_p(T_g)}{\lambda_g(T_g)} \quad (27)$$

Dynamic viscosity of propellant gases is calculated from the Sutherland equation [21]:

$$\mu_g(T_g) = 1.458 \cdot 10^{-6} \frac{T_g^{1.5}}{T_g + 110.33} \quad (28)$$

Gas thermal conductivity is given by relation [24]:

$$\lambda_g(T_g) = 1.317 \mu_g(T_g) \left[\frac{3540}{M} + c_p(T_g) \right] \quad (29)$$

The CFD simulation

Three types of heat transfer (conduction, convection and radiation) are considered in FLUENT simulation. All types are the result of internal flow of burning propellant grains and gaseous combustion products.

Conduction process is estimated by the energy equation, used in FLUENT for a solid material of a given geometry. The convective heat transfer coefficient is calculated from turbulent boundary layer and the P-1 heat radiation model is applied. More details are given in [25].

Temperature fields at the moment of reaching maximum nozzle surface temperature during firing with NC and NCD propellant are presented in fig. 7 and 8.

Experimental and calculated results of maximum nozzle inner surface temperature and corresponding time of reaching this temperature are given in tab. 4.

A good agreement of NERN and FLUENT computational results with measured maximum nozzle inner surface temperatures is obtained. From NERN code calculations a lower maximum temperatures and longer time of reaching these temperatures are obtained compared to the experimental values, while an opposite tendency appeared in FLUENT computational

results. Computational results obtained by NERN are slightly better. This can be attributed to the fact that two phase flow through the nozzle is taken into account only in the NERN code. However, a surface temperature distribution along the nozzle contour can be obtained only by FLUENT.

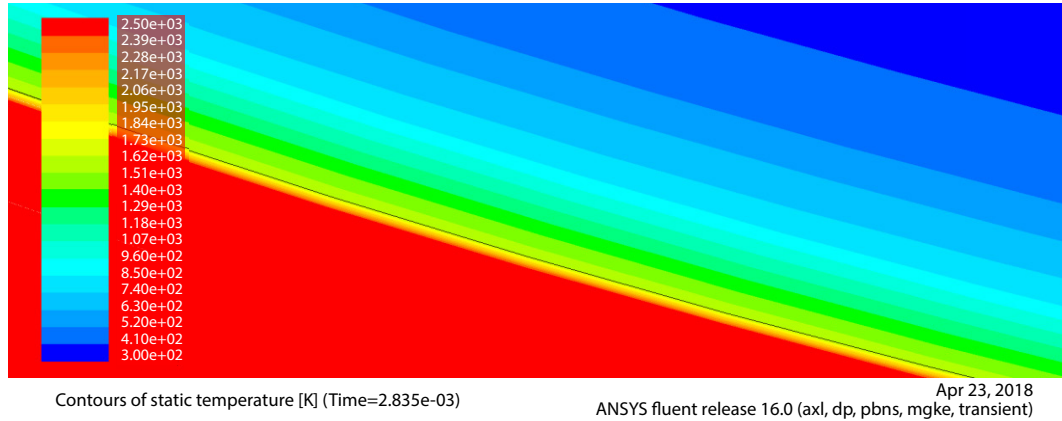


Figure 7. Temperature field at the moment of reaching maximum nozzle surface temperature during firing with NC propellant ($t_{w,max}=2.84$ ms)

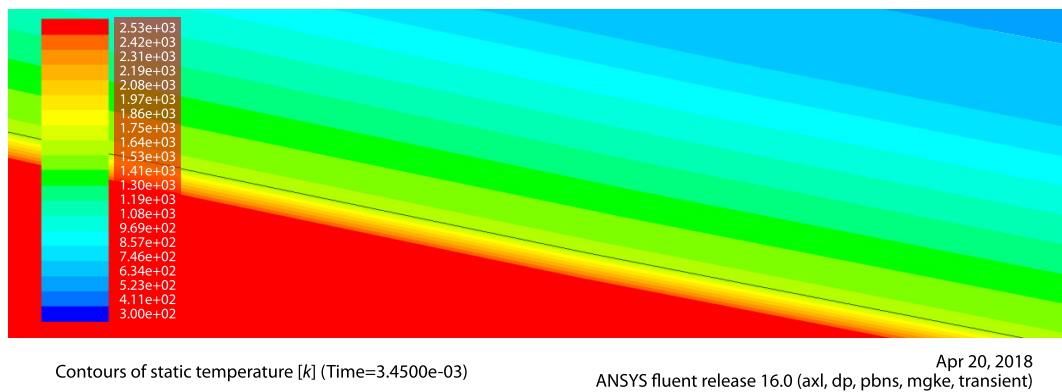


Figure 8. Temperature field at the moment of reaching maximum nozzle surface temperature during firing with NCD propellant ($t_{w,max}=3.45$ ms)

Table 4. Experimental and calculated maximum nozzle inner surface temperature and time of reaching this temperature

| Propellant | $T_{w,max}$ [K] | | | $t_{w,max}$ [ms] | | |
|------------|-----------------|------------------|--------------------|------------------|------------------|--------------------|
| | Experiment | NERN computation | FLUENT computation | Experiment | NERN computation | FLUENT computation |
| NC | 1576 | 1565 | 1593 | 3.08 | 3.37 | 2.84 |
| NCD | 1524 | 1484 | 1584 | 4.15 | 4.35 | 3.45 |

Discussion of results

Experimental results of groups A and B were used for analysing the influence of the layer of tungsten disulfide (WS_2) nanoparticles on nozzle erosion. Due to nano dimensions of

40-200 nm, these particles are going through the finest irregular surfaces of metal, creating a unique film and lubricant layer that provides low friction and reduced wear of surfaces treated with these particles. Resistance to high temperature of tungsten disulfide nanoparticles is exceptional and exceed 1470 K. Due to its structure of fullerene, nanoparticles possess outstanding mechanical properties and can withstand high levels of load and pressure. The layer of these particles was successfully applied in test barrels for 5.56×45 mm rifle in company *Prvi Partizan A. D.* [26]. Results in tab. 2 show that the presence of nanoparticles layer reduced nozzle erosion (90 mg mass loss in the first round compared to mean mass loss of 117 mg for group A). However, mean mass loss for rounds 2, 3, 4 and 5 of 116.5 mg (min. 114.2 mg; max. 118.6 mg) for group B, almost equal to 117 mg for group A, suggests that nanoparticles layer was removed from the nozzle surface during firing of first round. It seems that pressure and thermal loads of steel surface during firing are more severe in erosion device compared to the 5.56 mm rifle. In any case, experimentally determined maximum surface temperature is greater than limit temperature of nanoparticles resistance.

Experimental results of groups A and C were used for analysing the influence of propellant composition on gun steel erosion. Although the flame temperature of NCD propellant is more than 500 K lower from that of NC propellant, both propellants produced almost the same thermal load on the nozzle surface. Considerably greater nozzle erosion produced by group C cannot be explained by slightly greater pressure load produced by NCD propellant. In this case the mechanism exercised in the erosion device was primarily chemistry-driven modified material melt wipe in which the material had a considerably lowered melt temperature compared to the gun steel. The main reason for the higher erosivity of NCD over NC propellant is due to the composition of NCD, resulting in more CO production than that of NC, see tab. 3. The CO/CO₂ mass ratio for NCD is 5.92, while that for NC is 2.35. This additional CO makes more CO available on the nozzle surface for dissociation. The dissociated CO then provides free carbon for absorption in the steel lattice, and formation of iron carbides with considerably reduced melting temperature, 1423 K, than that of the gun steel with a melting temperature of about 1723 K. Similar conclusions were reported in [27].

Experimental results of groups C and D were used for analysing the influence of TiO₂/wax wear reducing additive in propellant charges on gun steel erosion.

In an attempt to retard the surface erosion in medium- and large-caliber guns, various materials, generally in the form of liners about the propellant bed, have been introduced into the propelling charge assembly. It has been experimentally observed during a gun firing that the use of these additives causes the bore surface temperature and heat input to the gun barrel to be reduced [28].

Experimental results obtained in erosion device and presented in tab. 2 show that TiO₂/wax additive decreased nozzle surface temperature and considerably reduced nozzle erosion. The erosion value for group D in tab. 2 is an average value based on a measurement taken after five shots, without cleaning of the nozzle between firings. A white residue and layer of gray coating were observed and removed before measurement of nozzle mass. This suggested that each shot was not equally erosive. In fact, during the first shot the solid particles of additive in the flow of propellant gases may reduce the turbulence level near the nozzle surface with the deposition on the surface. During each succeeding shot in the group the additive performs in the same manner, but the residue deposited as a coating from the previous shot may act as a passive thermal barrier, of thermal resistance to heat flow, additionally reducing erosion.

There are also some chemical mechanisms which may be important in reducing nozzle erosion. The additive may cause endothermic chemical reactions to occur within the

boundary-layer on the nozzle surface, or the coating deposited on the surface may inhibit the catalytic recombination of dissociated atomic species. In order to estimate the role of chemical mechanisms in decrease of nozzle erosion the Lawton's theory [30] of gun erosion is used. According to this theory the nozzle mass loss during firing in erosion device can be expressed:

$$m_{ER} = A \exp \frac{1.5 T_{w,max}}{B_0} \quad (30)$$

If chemical mechanisms involved by additive are insignificant, the coefficient of propellant erosivity, A , remains the same, so that for the same nozzle material the following equality comes from eq. (30) for experimental results of groups C and D:

$$\ln \frac{(m_{ER})_C}{(m_{ER})_D} = \frac{1.5}{B_0} [(T_{w,max})_C - (T_{w,max})_D] \quad (31)$$

From the results given in tab. 2 it follows that the left side of eq. (31) is equal to 0.565, while the right side is equal to 0.557. This indicates that TiO₂/wax additive may reduce nozzle erosion mainly by reducing the maximum surface temperature, without reducing propellant erosivity.

Experimental investigations of TiO₂/wax influence on gun barrel wear will soon be carried out by firings of real ammunition from 100 mm experimental gun. The wall temperature will be measured by micro thermocouples near the forcing cone of the gun bore. A measure of the barrel wear will be the change of gun bore dimensions.

Conclusions

Investigations concerning influence of various factors on gun steel erosion are carried out by firings in erosion device based on modification of 37 mm M39 gun. The factors are mainly related to the thermal load of nozzle inside surface.

The nozzle mass loss during firing was the measure of gun steel erosion.

The maximum nozzle inner surface temperature was determined experimentally by micro thermocouples measurements at specified distance away from the inner surface and by solution of the inverse heat conduction problem.

Modelling of propellant combustion products flow and heat transfer to the nozzle were conducted using developed 1-D interior ballistic code with heat transfer (NERN code) and CFD simulation by the commercial FLUENT program. A very good compatibility of experimental and computational results of pressure profile during firings in erosion device and maximum nozzle inner surface temperature was achieved. Slightly better results were obtained with NERN code, due to taking into account the two phase flow through the nozzle after bursting of the disk.

Influence on nozzle erosion of tungsten-disulfide nanoparticles layer, different propellant types and TiO₂/wax wear reducing liner in the propellant charge was analysed.

There are indications that IF-WS₂ layer can protect the nozzle surface from erosion in certain degree, but it is necessary to consider other ways of layer application, because in this research it was carried away after the first round.

In spite of lower thermal load of the nozzle a higher erosivity was observed for NC propellant than for NCD propellant. The main reason for this is the composition of NC, resulting in more CO production than that of NCD.

It was observed that TiO₂/wax wear reducing additive considerably reduced nozzle erosion. The additive decreased nozzle surface temperature without reducing propellant erosivity.

Experimental investigations of TiO₂/wax influence on gun barrel wear will soon be carried out by firings of real ammunition from 100 mm experimental gun.

Nomenclature

| | |
|---------------|--|
| A | – coefficient of propellant erosivity [mg] |
| B_0 | – hot hardness coefficient of gun steel, 377 [K] |
| c | – specific heat, [Jkg ⁻¹ K ⁻¹] |
| c_p | – specific heat at constant pressure, [Jkg ⁻¹ K ⁻¹] |
| c_v | – specific heat at constant volume, [Jkg ⁻¹ K ⁻¹] |
| D_h | – hydraulic diameter, [m] |
| d | – nozzle throat diameter, [m] |
| d_{eq} | – equivalent diameter of propellant grain, [m] |
| f | – force (impetus), [Jkg ⁻¹] |
| h | – coefficient of convective heat transfer, [Wm ⁻² K ⁻¹] |
| l_{th} | – thermocouple distance from nozzle inside surface, [m] |
| M | – molar mass of propellant gases, [kgkmol ⁻¹] |
| m | – mass [kg] |
| m_{ER} | – nozzle mass loss per round, [mg] |
| m_{WRA} | – mass of wear reducing additive, [kg] |
| \dot{m} | – mass-flow rate [kgs ⁻¹] |
| p | – pressure of propellant gases, [Pa] |
| Q_{car} | – heat transferred to the cartridge, [J] |
| Q_{noz} | – heat transferred to the nozzle, [J] |
| q | – heat flux [Wm ⁻²] |
| R | – gas constant, [Jkg ⁻¹ K ⁻¹] |
| \mathcal{R} | – universal gas constant, 8314 [Jkmol ⁻¹ K ⁻¹] |
| r | – propellant burning rate [ms ⁻¹] |
| S | – burning surface area of propellant grain, [m ²] |
| T | – temperature, [K] |
| T_f | – flame temperature, [K] |
| t | – time, [s] |
| V | – volume of propellant grain, [m ³] |

| | |
|-------|---|
| W_0 | – chamber volume of erosion device, [m ³] |
| x | – coordinate normal to the wall surface, [m] |

Greek letters

| | |
|---------------|---|
| α | – thermal diffusivity, [m ² s ⁻¹] |
| β | – co-volume of propellant gases, [m ³ kg ⁻¹] |
| δ | – thermal wave depth, [m] |
| ε | – emissivity of the nozzle wall, [–] |
| ϕ | – porosity, [–] |
| γ | – propellant mass fraction in mixture, [–] |
| η | – mass fraction of propellant gases flowing out of nozzle, [–] |
| κ | – specific heat ratio (= c_p/c_v), [–] |
| λ | – thermal conductivity, [Wm ⁻¹ K ⁻¹] |
| μ | – dynamic viscosity, [kgm ⁻¹ s ⁻¹] |
| ρ | – density, [kgm ⁻³] |
| σ_{SB} | – Stefan-Boltzmann constant, (= 5.670373 · 10 ⁻⁸) [Wm ⁻² K ⁻⁴] |
| ψ | – mass fraction of burned propellant, [–] |
| ζ | – mass fraction of unburned propellant flowing out of nozzle, [–] |

Subscripts

| | |
|-----|-----------------|
| c | – convection |
| g | – gas |
| i | – igniter |
| m | – mixture |
| max | – maximum |
| n | – nozzle |
| pr | – propellant |
| r | – radiation |
| w | – wall surface |
| 0 | – initial value |

References

- [1] Ahmad, I., The Problem of Gun Barrel Erosion: An Overview, in: *Gun Propulsion Technology*, (Ed. M. Summerfield), Progress in Astronautics and Aeronautics, AIAA, Reston, Va., USA, 1988, Vol. 109, pp. 311-356
- [2] Ebihara, W. T., Rorabaugh D. T., Mechanisms of Gun-Tube Erosion and Wear, in: *Gun Propulsion Technology*, (Ed. M. Summerfield), Progress in Astronautics and Aeronautics, AIAA, Reston, Va., USA, 1988, Vol. 109, pp. 357-376
- [3] Bracuti, A., J., Wear-Reducing Additives – Role of the Propellant, in: *Gun Propulsion Technology*, (Ed. M. Summerfield), Progress in Astronautics and Aeronautics, AIAA, Reston, Va., USA, 1988, Vol. 109, pp. 377-412
- [4] Sopok, S., *et al.*, Thermal-Chemical-Mechanical Gun Bore Erosion of an Advanced System – Part I: Theories and Mechanisms, *Wear*, 258 (2005), 1-4, pp. 659-670
- [5] Sopok, S., *et al.*, Thermal-Chemical-Mechanical Gun Bore Erosion of an Advanced System – Part II: Modelling and Predictions, *Wear*, 258 (2005), 1-4, pp. 671-683

- [6] Jaramaz, S., Micković, D., Simulation of Gun Tube Erosion (in Serbian), *Scientific Technical Review*, 40 (1990), 8-9, pp. 35-41
- [7] Adžić, M., et al., Determination of Inner Surface Gun Bore Temperature (in Serbian), *Scientific Technical Review*, 45 (1997), 5-6, pp. 70-73
- [8] Adžić, M., et al., Design of Dedicated Instruments for Temperature Distribution Measurements in Solid Oxide Fuel Cells, *Journal of Applied Chemistry*, 27 (1997), 12, pp. 1355-1361
- [9] Carasso, A., Determining Surface Temperatures from Interior Observations, *SIAM Journal of Applied Mathematics*, 42 (1982), 3, pp. 558-574
- [10] Carasso, A., Non-Linear Inverse Heat Transfer Calculations in Gun Barrels, Report ARO 19643.1-MA, Center for Applied Mathematics, National Bureau of Standards, Washington DC, 1983
- [11] Versteegen, P. L., Varcolik, F., D., Heat Transfer Studies in Gun Tubes, Report BRL-CR-00393, Ballistic Research Laboratory, Aberdeen Proving Ground, Md., USA, 1979
- [12] Gerber, N., Bundy, M., Effect of Variable Thermal Properties on Gun Tube Heating, Report BRL-MR-3984, Ballistic Research Laboratory, Aberdeen Proving Ground, MD, USA, 1992
- [13] Jaramaz, S., et al., Determination of gun propellant erosivity: Experimental and theoretical studies, *Experimental Thermal and Fluid Science*, 34 (2010), 6, pp. 760-765
- [14] Boisson, D., et al., Experimental Investigation of Heat Transfer in a 120 mm Testing Gun Barrel Based on a Space Marching Finite Difference Algorithm for the Inverse Conduction Method, *Proceedings*, 19th International Symposium on Ballistics, Interlaken, Switzerland, 2001, pp. 163-170
- [15] ***, Fluent Inc., FLUENT 5 User's Guide, 1998
- [16] Micković, D., Jaramaz, S., NERT – Computer Code for Nozzle Erosion in Vented Chamber (in Serbian), Weapon Systems Department, Faculty of Mechanical Engineering, Report No 3/2007, Belgrade, 2007
- [17] Micković, D., Jaramaz, S., TCC – Computer Code for Thermo-Chemical Calculations (in Serbian), Report No 1/1996, Weapon Systems Department, Faculty of Mechanical Engineering, Belgrade, 1996
- [18] Cvetinović, D., et al., Review of the Research on the Turbulence in the Laboratory for Thermal Engineering and Energy, *Thermal Science*, 21 (2016), Suppl. 3, pp. S875-S898
- [19] Weinacht, P., Conroy, P., A Numerical Method for Predicting Thermal Erosion in Gun Tubes, Report ARL-TR-1156, Army Research Laboratory, Aberdeen Proving Ground, Md., USA, 1996
- [20] Dorignac, E., Vullierme, J., Error Resulting from the Surface Conduction Effects when Determining Surface Transfers by Thin Wall or Semi-infinite Wall Methods, *La Recherche Aérospatiale*, 1 (1991), Jan., pp. 67-73
- [21] Woodley, C., et al., QinetiQ Studies on Wear and Erosion in Gun Barrels, in: *The Control and Reduction of Wear in Military Platforms*, RTO-MP-AVT-109, 2004, NATO, Washington DC, pp. 15-1-15-12
- [22] Nelson, W. C., Ward, J. R., Calculation of Heat Transfer to the Gun Barrel Wall, *Journal of Ballistics*, 6 (1982), 3, pp. 1518-1524
- [23] Horst, A., W., The Influence of Propellant Grain Shape, Size, and Composition on Solid Phase Motion and Heat Transfer to the Gun Tube, *Proceedings*, 26th International Symposium on Ballistics, Miami, Fla., USA, 2011, pp. 12-16
- [24] Jojić, B., et al., *Manual for the Design of Probing Rockets – Volume II Propulsion Group* (in Serbian), SAROJ, Belgrade, 1978
- [25] Živković, S., et al., Experimental and Simulation Testing of Thermal Loading in the Jet Tabs of a Thrust Vector Control System, *Thermal Science*, 20 (2016), Suppl. 1, pp. S275-S286
- [26] Erčević, M., et al., Applying of Nanotechnology in Production of Rifle Ammunition, *Proceedings*, 7th International Conference on Defensive Technologies OTEH, Belgrade, 2016, pp. 260-265
- [27] Conroy, P., Vented Fixture Modeling, Report ARL-TR-2952, Army Research Laboratory, Aberdeen Proving Ground, Md., USA, 2003
- [28] Brosseau, T., L., Ward, R., Measurement of Heat Input into the 105 mm M68 Tank Cannon Firing Rounds Equipped with Wear-Reducing Additives, Report BRL-TR-02056, Ballistic Research Laboratory, Aberdeen Proving Ground, Md., USA, 1978
- [29] Lawton, B., Thermal and Chemical Effects on Gun Barrel Wear, *Proceedings*, 8th International Symposium of Ballistics, Orlando, Fla., USA, 1984, pp. II-28-II-36